

Article

On the numerical simulation of HPDEs using θ -weighted scheme and the Galerkin method

Haifa Bin Jebreen ^{1,†,*} , Fairouz Tchier ^{2,†}¹ Department of mathematics, college of science, King Saud university, KSA ; hjebeen@ksu.edu.sa² Department of mathematics, college of science, King Saud university, KSA ; ftchier@ksu.edu.sa

* Correspondence: hjebeen@ksu.edu.sa

† These authors contributed equally to this work.

Version December 6, 2020 submitted to Journal Not Specified

Abstract: Herein, an efficient algorithm is proposed to solve one dimensional hyperbolic partial differential equation. In order to reach an approximate solution of such equation, we employed the θ -weighted scheme to discretize the time interval into a finite number of time steps. In each of the steps, we have a linear ordinary differential equation. To solve this equation, we utilized the Galerkin method based on interpolating scaling functions. Therefore in each time steps, the solution can be found as a continuous function. The stability, consistency and convergency of the proposed method investigated. Several numerical examples are devoted to show the accuracy and efficiency of the method and guarantee the validity of the stability, consistency, and convergence analysis.

Keywords: Interpolating scaling functions; Hyperbolic equation; Galerkin method

1. Introduction

Partial differential equations (PDEs) are ubiquitous in mathematically scientific fields and play an important role in engineering and physics. They arise from many purely mathematical considerations, such as the calculus of variations and differential geometry. One of the momentous subclasses of PDEs is the hyperbolic partial differential equations (HPDEs). HPDEs are used to model many phenomena such as biology, industry, atomic physics, aerospace[4,7,11]. Telegraph and wave equations are the most famous type of HPDEs that are enforceable in various fields such as random walk theory, wave propagation, and signal analysis [7,10].

In this study, we construct and analyze a numerical algorithm based on the finite difference method, especially the θ -weighted method, and the Galerkin method is proposed to solve the HPDEs of form

$$w_t(x, t) + a_1 w_x(x, t) + a_2 w(x, t) = f(x, t), \quad x \in [0, 1], t \in [0, T], \quad (1)$$

with boundary condition

$$w(0, t) = g(t), t \in [0, T], \quad (2)$$

and initial condition

$$w(x, 0) = h(t), x \in [0, 1]. \quad (3)$$

Further, we assume that f , g , and h are the known functions, and also a_1 and a_2 are the real value constants.

In this paper, we attempt to apply an efficient scheme that has not been used before to solve such problems. The method includes three steps. In the first step, we use the θ -weighted method to broke the time interval into a finite number of time steps. At each time step, we obtain a linear ordinary differential equation. In the second step, the ODE obtained from the first step is solved

24 using the Galerkin method. To do this, interpolating scaling functions are used. In comparison
 25 to the scaling function arisen from multiresolution analysis (MRA), interpolation scaling functions
 26 have properties that make them attractive. These characteristics include the flexible zero moments, a
 27 compact support, orthonormality, and having a closed-form. The most important property of these
 28 bases is the interpolation. This property is useful to avoid integrals to find coefficients in expansions.
 29 At the last step, the linear algebraic system obtained from the second one must be solved using an
 30 appropriate technique. Stability, consistency, and convergence analysis are investigated, and numerical
 31 tests guarantee the validity of them.

32 Numerous studies proposed a variety of numerical and analytical solutions to HPDEs. Doha et
 33 al. [8] proposed a numerical method based on the collocation method for solving a system consist of
 34 such equations. In [9], the spectral-Galerkin method is proposed to solve this equation. Singh et al.
 35 [16] solved one dimensional HPDEs with the initial and boundary conditions, (2) and (3) utilizing a
 36 algorithm based on Chebyshev and Legendre multiwavelets. Dehghan et al. [5] introduced a numerical
 37 scheme based on the cubic B-spline scaling functions to solve (1) with nonlocal conservation condition.
 38 Bin Jebreen et al. [10] proposed an efficient method based on wavelet Galerkin method to solve the
 39 Telegraph equation, and also the collocation method based on interpolating scaling functions is used
 40 for solving this equation in [11]. for more study, we refer the readers to [3,6].

41 The outline of the remaining part of the paper is as follows. Section 2 is devoted to the brief
 42 introduction to the interpolating scaling function. Mixed θ -weighted scheme and Galerkin method
 43 based on interpolating scaling functions is used to solve the desired equation and also the stability,
 44 consistency and convergence analysis are investigated in Section 3. Section 4 is devoted to some
 45 numerical examples to show the ability and accuracy of the method.

46 2. Interpolating scaling functions

To derive a set of bases that possess the multiresolution analysis conditions, Alpert et al. [1]
 introduced a set of functions that generates the nested spaces $\{V_j^r\}_{j=0}^\infty \in L_2[0,1]$ using piecewise
 polynomial bases of degree less than $r \geq 0$ (the multiplicity parameter). Considering $\mathcal{B} := \{0, \dots, 2^j - 1\}$,
 and $\mathcal{R} := \{0, 1, \dots, r-1\}$, there is a sequence of nested subspaces that are spanned by

$$V_j^r := \text{Span}\{\phi_{j,b}^k := \phi^k(2^j x - k), b \in \mathcal{B}_j, k \in \mathcal{R}\} \subset L_2(\Omega), \quad r \geq 0, \quad j \in \mathbb{Z}^+ \cup \{0\},$$

by means of the Interpolating scaling functions (ISFs) $\{\phi^k\}_{k \in \mathcal{R}}$ introduced by Alpert using the Legendre
 polynomials $\{L_k(t)\}_{k \in \mathcal{R}}$ of degree r , at the roots $\{\tau_k\}_{k \in \mathcal{R}}$ of $L_r(t)$. Given $\{\omega_k\}_{k \in \mathcal{R}}$ which are the
 Gauss-Legendre quadrature weights [1,11] ISFs are defined as follows

$$\phi^k(x) = \begin{cases} \sqrt{\frac{2}{\omega_k}} L_k(2x-1), & x \in [0,1], \\ 0, & o.w. \end{cases}$$

47 These bases fulfill the orthonormality relation $\langle \phi_{j,b}^k, \phi_{j,b'}^{k'} \rangle = \delta_{b,b'} \delta_{k,k'}$ where $\langle \cdot, \cdot \rangle$ denotes the L_2 -inner
 48 product on $\Omega := [0,1]$.

Assume that $\cup_{b \in \mathcal{B}} I_{j,b}$ is a uniform finite discretization of Ω . Here the subinterval $I_{j,b} := [x_b, x_{b+1}]$
 are specified by points $x_b := b/(2^j)$. To project a function into V_j^r , we introduce the orthogonal
 projection \mathcal{P}_j^r that maps $L^2(\Omega)$ onto the subspace V_j^r . Utilizing this projection, every function $p \in L^2(\Omega)$
 can be represented in the form

$$p \approx \mathcal{P}_j^r(p) = \sum_{b \in \mathcal{B}_j} \sum_{k \in \mathcal{R}} p_{j,b}^k \phi_{j,b}^k. \quad (4)$$

Due to the orthonormality of the bases, it is easy to prove that the coefficients $p_{j,b}^k$ can be obtained by $\langle p, \phi_{j,b}^k \rangle = \int_{I_{j,b}} f(x) \phi_{j,b}^k(x) dx$. To avoid integration, we apply the interpolation property of ISFs [1,12], via

$$p_{j,b}^k \approx 2^{-J/2} \sqrt{\frac{\omega_k}{2}} p \left(2^{-J} \left(\frac{\tau_k + 1}{2} + b \right) \right), \quad b \in \mathcal{B}_J, k \in \mathcal{R}. \quad (5)$$

Given r -times continuously differentiable function $p \in \mathbb{C}^r(\Omega)$, the projection $\mathcal{P}_J^r(p)$ is bounded by means of L_2 -inner product as

$$\|\mathcal{P}_J^r(p) - p\| \leq 2^{-Jr} \frac{2}{4^r r!} \sup_{x \in [0,1]} |p^{(r)}(x)|. \quad (6)$$

49 According to this relation, this projection is convergent when J or r increases. To study more details,
50 we refer the readers to [2]. Consequently, this projection is convergent with the rate of $O(2^{-Jr})$.

We determine the vector function $\Phi_J^r := [\Phi_{r,J,0}, \dots, \Phi_{r,J,2^J-1}]^T$ with $\Phi_{r,J,b} := [\phi_{J,b}^0, \dots, \phi_{J,b}^{r-1}]$ includes the scaling functions and called multi-scaling function. The approximation (4) can be rewritten using the vector P whose entries are $P_{br+k+1} := p_{j,b}^k$ as follows

$$\mathcal{P}_J^r(p) = P^T \Phi_J^r, \quad (7)$$

51 where P is a vector of dimensional $N := r2^J$.

To approximate a higher-dimensional function, the building blocks of the bases can be utilized. In this regards, one can consider the subspace $V_J^{r,2} := V_J^r \times V_J^r \subset L^2(\Omega \times \Omega)$ that is spanned by

$$\{\phi_{j,b}^k \phi_{j,b'}^{k'} : b, b' \in \mathcal{B}_J, k, k' \in \mathcal{R}\}.$$

In order to derive an approximation of two-dimensional function $p \in L^2(\Omega \times \Omega)$, we apply the projection operator \mathcal{P}_J^r , viz

$$p(s, t) \approx \mathcal{P}_J^r(p)(x, t) = \Phi_J^{rT}(x) P \Phi_J^r(t), \quad (8)$$

where components of the square matrix P of order N are obtained by

$$P_{rb+(k+1),rb'+(k'+1)} \approx 2^{-J} \sqrt{\frac{\omega_{k'}}{2}} \sqrt{\frac{\omega_k}{2}} p \left(2^{-J} (\hat{\tau}_k + b), 2^{-J} (\hat{\tau}_{k'} + b') \right), \quad (9)$$

where $\hat{\tau}_k = (\tau_k + 1)/2$. If $C^{(2r)}(\Omega \times \Omega) \ni p : \Omega \times \Omega \rightarrow \mathbb{R}$, we can show that the error arose from this approximation can be bounded as follows

$$\|\mathcal{P}_J^r p - p\| \leq \mathcal{M}_{\max} \frac{2^{1-rJ}}{4^r r!} \left(2 + \frac{2^{1-Jr}}{4^r r!} \right), \quad (10)$$

where \mathcal{M}_{\max} is a constant [12]

$$\mathcal{M}_{\max} = \max \left\{ \sup_{\xi \in [0,1]} \left| \frac{\partial^r}{\partial x^r} p(\xi, y) \right|, \sup_{\eta \in [0,1]} \left| \frac{\partial^r}{\partial y^r} p(x, \eta) \right|, \sup_{\xi', \eta' \in [0,1]} \left| \frac{\partial^{2r}}{\partial x^r \partial y^r} p(\xi', \eta') \right| \right\}.$$

52 3. Numerical method of solution

53 The main idea behind the proposed method is based on the θ -weighted scheme and Galerkin
54 methods. In the first step, the θ -weighted method is used to discretize the time interval into a finite
55 number of time steps. The linear system of ordinary differential equations obtained after the first step
56 can be reduced to a system of algebraic equations by using the Galerkin method in the second one.
57 So, one can find the approximate solution of the desired equation at the time step points $t_n := n\delta t$,
58 $n = 0, \dots, M$ ($t_n \in [0, T]$ and $T = M\delta t$).

To discretize the time variable, a finite difference discretization for (1), the theta weighted discretization is then

$$\frac{w^{n+1} - w^n}{\delta t} + \theta (a_1 w_x^{n+1} + a_2 w^{n+1}) + (1 - \theta) (a_1 w_x^n + a_2 w^n) = f(x, t^n) + \mathfrak{R}, \quad (11)$$

59 where for simplicity $w(x, t + n\delta t)$ is assumed to be w^n , for $t^n = t^{n-1} + \delta t$ (or equivalently $t^n = n\delta t$),
60 and also $\mathfrak{R} \leq \mathfrak{C}\delta t$ for a positive constant \mathfrak{C} and $\theta \in [0, 1]$ is a constant. Note that by selecting the
61 different values for θ , one can find various methods, such as implicit method ($\theta = 1$), explicit method
62 ($\theta := 0$), and the Crank–Nicolson method ($\theta = 1/2$).

Since the remainder term \mathfrak{R} is a small quantity, one can neglect it and after simplification writes

$$w^{n+1} + \theta\delta t (a_1 w_x^{n+1} + a_2 w^{n+1}) = w^n - (1 - \theta)\delta t (a_1 w_x^n + a_2 w^n) + \delta t f(x, t^n), \quad n = 0, \dots, M. \quad (12)$$

Next, this system of ordinary differential equations would be discretized by the Galerkin method based on ISFs. To this end, one can approximate the solution w^n of (12) using projection operator \mathcal{P}_f^r , via,

$$w^n(x) \approx \mathcal{P}_f^r(w^n)(x) = W_n^T \Phi_f^r(x), \quad n = 0, \dots, M, \quad (13)$$

where W_n , for $n = 1, \dots, M$ is a vector with dimension N which must be found. The same approximation could be imagined to w_x^n , as

$$w_x^n(x) \approx \mathcal{P}_f^r(w_x^n)(x) = W_n^T D_\phi \Phi_f^r(x), \quad n = 0, \dots, M, \quad (14)$$

63 where D_ϕ is the operational matrix for derivative introduced in [13–15].

Replacing (13) and (14) in (12), yields

$$\left(W_{n+1}^T + \theta\delta t (a_1 W_{n+1}^T D_\phi + a_2 W_{n+1}^T) \right) \Phi_f^r(x) = \left(W_n^T - (1 - \theta)\delta t (a_1 W_n^T D_\phi + a_2 W_n^T) + \delta t F_n^T \right) \Phi_f^r(x), \quad (15)$$

where F_n is a $N \times 1$ vector which is obtained by projecting the function f^n into V_f^r , viz

$$f^n \approx \mathcal{P}_f^r(f^n)(x) = F_n^T \Phi_f^r(x), \quad n = 0, \dots, M.$$

Let

$$\begin{aligned} A^T &:= (1 + a_2\theta\delta t)I + a_1\theta\delta t D_\phi, \\ b^T &:= W_n^T ((1 - a_2(1 - \theta)\delta t)I - a_1(1 - \theta)\delta t D_\phi) + \delta t F_n^T, \quad n = 0, \dots, M, \end{aligned} \quad (16)$$

where I is identity matrix of dimension N . By these assumptions and using the fact that the entries of vector $\Phi_f^r(x)$ are orthonormal bases for V_f^r . So they are linearly independent, and then we have the following system of a linear system

$$AW_{n+1} = b. \quad (17)$$

To apply the boundary condition (2), it can also be projected into V_f^r , via

$$w^{n+1}(0) \approx W_{n+1}^T \Phi_f^r(0) = g(t^{n+1}). \quad (18)$$

Substituting the first row of A and the first element of b by $\Phi_f^r(0)^T$ and $g(t^{n+1})$, respectively, we obtain the modified system

$$\tilde{A}W_{n+1} = \tilde{b}. \quad (19)$$

Now, note that to start the steps, the initial condition should be utilized via

$$w(x, 0) \approx W_0^T \Phi_f^r(x) = H^T \Phi_f^r(x), \quad (20)$$

and then $W_0 = H$ where H is a vector of dimension N . Utilizing $W_0 = H$, equation (19) gives a system of equations at every time steps t^n , $n = 0, \dots, M$. So one can obtain the approximate solution $w(x, t^n)$ by means of a linear expansion of interpolating scaling function (13).

3.1. Stability

To analyze the stability of the time discretization by θ -weighted scheme, assume that \hat{u}_{n+1} is the approximation solutions of (17). We set $e^{n+1} := w^{n+1} - \hat{w}^{n+1}$ as the error that arises from the proposed Galerkin method. Consequently, the roundoff error can be obtained via

$$(1 + a_2\theta\delta t)e^{n+1} + a_1\theta\delta te_x^{n+1} = (1 - a_2(1 - \theta)\delta t)e^n - a_1(1 - \theta)\delta te_x^n. \quad (21)$$

Projecting the error e^n using \mathcal{P}_J^r , one can write

$$e^n \approx \mathcal{P}_J^r(e^n) = E_n^T \Phi_J^r. \quad (22)$$

Inserting (22) into (21) and applying the operational matrix of derivative for ISFs, we get

$$\Phi_J^{rT} A E_{n+1} = \Phi_J^{rT} B E_n, \quad (23)$$

where $B^T := (1 - a_2(1 - \theta)\delta t)I - a_1(1 - \theta)\delta t D_\phi$. Provided the matrices A is inverted, it can be shown

$$E_{n+1} = A^{-1} B E_n. \quad (24)$$

Taking the norm of both sides of (24), and using matrix norm property, we obtain the following inequality

$$\|E_{n+1}\| \leq \|A^{-1}B\| \|E_n\|, \quad n = 0, \dots, M. \quad (25)$$

This gives rise to a sufficient and necessary condition for the stability of the method so that to have a stable method, the spectral radius of the matrix $A^{-1}B$ must be less than one ($\rho < 1$ where ρ is a spectral radius of $A^{-1}B$).

3.2. Convergence analysis

Assume that $e^{n+1} := w^{n+1} - \hat{w}^{n+1}$. Subtracting (12) from (15) and using the notations in the previous section, one can write after some simplification

$$\|E_{n+1}\| \leq \|A^{-1}\| \|B\| \|E_n\| + \|A^{-1}\| \|f^n - \hat{f}^n\|, \quad (26)$$

where $f^n := f(x, t^n)$ and $\hat{f}^n := \mathcal{P}_J^r(f^n)$. Due to invertibility of matrix D_ϕ [1], it is obvious that $C_1 := \|A^{-1}\|$ and $C_2 := \|B\|$ are finite. Therefore, we have

$$\|E_{n+1}\| \leq C_1 \left(C_2 \|E_n\| + \|f^n - \hat{f}^n\| \right).$$

It follows from (6) that $\|E_n\|$ and $\|f^n - \hat{f}^n\|$ are bounded and it gives the result that

$$\|e^{n+1}\| \leq C_1 \frac{2^{1-Jr}}{4^r r!} \left(C_2 \sup_{x \in [0,1]} |w^{n(r)}(x)| + \sup_{x \in [0,1]} |f^{n(r)}(x)| \right). \quad (27)$$

Note that θ plays an important role in matrices A^{-1} and B . So the value of the variables C_1 and C_2 will change when the value of θ changes. These variables play a direct role in the error presented in (27).

We know that a method is consistent if by reducing the mesh (by increase the refinement level J) and time step size (δt), the truncation error terms could be made to approach zero. Consequently The

Table 1. Comparison of L_2 -error computed using explicit, implicit and Crank–Nicolson methods with time step size $\delta t = 0.1/2^{m-1}$ for Example 1.

θ	$m = 1$	$m = 2$	$m = 3$	$m = 4$	$m = 5$	$m = 6$	$m = 7$	$m = 8$	$m = 9$	$m = 10$
0	$1.18e + 4$	$4.33e + 6$	$3.10e + 7$	$7.57e + 4$	2.95	$1.22e - 3$	$1.39e - 4$	$6.80e - 5$	$3.39e - 5$	$1.69e - 5$
1/2	$3.4e - 2$	$1.7e - 2$	$8.5e - 3$	$4.2e - 3$	$2.1e - 3$	$1.0e - 3$	$5.1e - 4$	$2.5e - 4$	$1.3e - 4$	$8.2e - 5$
1	$5.8e - 2$	$2.9e - 2$	$1.5e - 2$	$7.3e - 3$	$3.7e - 3$	$1.8e - 3$	$9.0e - 4$	$4.4e - 4$	$2.1e - 4$	$1.1e - 4$

76 inequality (27) confirms that the method is consistent at every time steps when the refinement level J
77 or multiplicity r increases.

78 If the condition for stability holds ($\rho(A^{-1}B) < 1$) and if the Galerkin method, used for solving
79 the ordinary differential equation at each time, approaches to zero as $J \rightarrow \infty$ (indeed the method is
80 consistent), we usually find that the solution converges to the exact solution. This derives from Lax
81 Equivalence Theorem.

82 4. Numerical results

83 To illustrate the validity of stability, consistency, and convergence analysis, some numerical tests
84 have been considered in this section.

Example 1. Let us dedicate the first example to the case that the desired equation (1) is of form

$$w_t(x, t) + w_x(x, t) + w(x, t) = -2 \sin(x + t) + \cos(x + t),$$

with boundary and initial conditions are given by

$$w(x, 0) = \cos(x), \quad x \in [0, 1], \quad w(0, t) = \cos(t), \quad t \in [0, T].$$

One can find the exact solution that is reported in [9]

$$w(x, t) = \cos(x + t).$$

85 Table 1 describes the comparison of L_2 -error via explicit, implicit and Crank–Nicolson methods with time
86 step size $\delta t = 0.1/2^{m-1}$, $m = 1, \dots, 10$. It is quite obvious that the error tends to zero with increasing m . Table
87 3 consist of L_2 norm of example 1 at different values of time. The L_2 -error graph of the explicit, implicit, and
88 Crank–Nicolson methods taking different values for J when $r = 3$ are shown in Figure 3. Figure 4 illustrate the
89 approximate solution and absolute error taking $r = 5$ and $J = 2$ at time $t = 1$. Table 4 displays absolute values
90 of the error at the selected points by using the presented method taking $r = 4$, $J = 1$, $\theta = 1/2$ and $\delta t = 0.1/2^9$.
91 The results have been compared with the Legendre wavelets and Chebyshev wavelet collocation method [16],
92 and also Bernoulli matrix approach [17]. To confirm the stability condition that we obtained in subsection 3.1,
93 Figures 1, 2 and Table 1 are considered. One can observe that when the spectral radius of matrix $A^{-1}B$ is less
94 than 1, the proposed method is stable. In view of Figures 1, and 2, the explicit method at $m = 10$ becomes stable
95 while the Crank-Nicolson method is stable from $m = 1$. We have the same result for the implicit method ($\theta = 1$).

Example 2. As the second example, let us to consider the HPDEs (1) so that $a_1 = 1$, $a_2 = 1$ and

$$f(x, t) = (x - t)^2,$$

with boundary and initial conditions are given by

$$w(x, 0) = x^2, \quad x \in [0, 1], \quad w(0, t) = t^2, \quad t \in [0, T].$$

Table 2. L^2 norm of errors taking $r = 5, J = 2, \theta = 1/2$ and $\delta t = 0.1/2^{m-1}$ for Example 1.

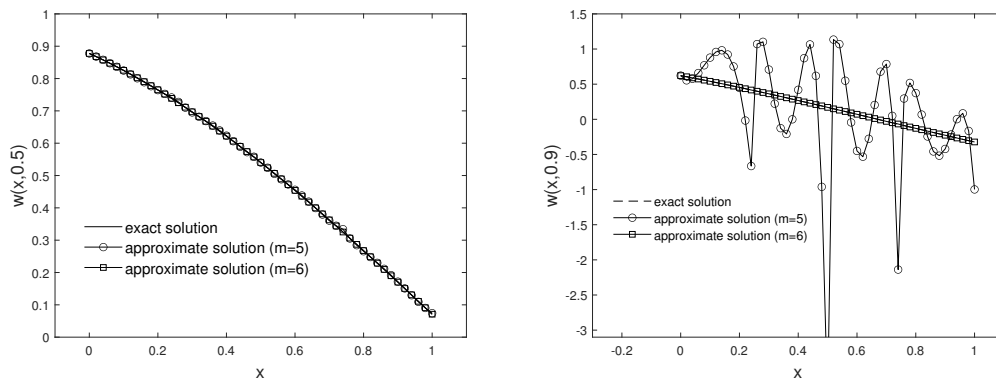
m	$\theta = 0$	$\theta = 0.5$	$\theta = 1$
1	2.74556398	0.99667345	0.95750928
2	1.96489325	0.99446140	0.97722388
3	1.45253127	0.99335639	0.98830702
4	1.16631074	0.99488512	0.99408949
5	1.04801504	0.99716602	0.99704939
6	1.01190091	0.99850952	0.99855537
7	1.00262776	0.99928905	0.99930055
8	1.00046389	0.99965462	0.99965498
9	1.00001839	0.99982309	0.99982817
10	0.99995576	0.99991242	0.99991142

Table 3. L^2 norm of errors taking $r = 5, J = 2, \theta = 1/2$ and $\delta t = 0.1/2^{m-1}$ for Example 1.

m	$t = 0.2$	$t = 0.4$	$t = 0.6$	$t = 0.8$	$t = 1.0$
2	$9.07e-3$	$1.50e-2$	$1.80e-2$	$1.86e-2$	$1.71e-2$
4	$2.27e-3$	$3.74e-3$	$4.50e-3$	$4.63e-3$	$4.24e-3$
6	$5.67e-4$	$9.34e-4$	$1.12e-3$	$1.16e-3$	$1.06e-3$
8	$1.42e-4$	$2.34e-4$	$2.81e-4$	$2.89e-4$	$2.65e-4$
10	$3.54e-5$	$5.84e-5$	$7.02e-5$	$7.23e-5$	$6.63e-5$

Table 4. Absolute values of the error at the selected points taking $\theta = 1/2$ and $\delta t = 0.1/2^9$ for Example 1.

(x, t)	[16] ($M = M' = 4$)		[17] ($N = 4$)	Proposed method
	Legendre wavelets	Chebyshev wavelet		$r = 4, J = 1$
(0.1, 0.1)	$4.86e-5$	$3.0e-4$	$3.220e-5$	$5.332e-6$
(0.2, 0.2)	$2.78e-4$	$2.0e-4$	$6.650e-5$	$6.791e-6$
(0.3, 0.3)	$8.64e-5$	$1.0e-4$	$1.357e-4$	$4.366e-5$
(0.4, 0.4)	$1.15e-4$	$5.0e-4$	$1.332e-4$	$1.505e-4$
(0.5, 0.5)	$1.42e-4$	$6.0e-4$	$5.200e-5$	$1.509e-4$
(0.6, 0.6)	$5.40e-6$	$2.0e-4$	$7.700e-5$	$1.992e-4$
(0.7, 0.7)	$1.67e-4$	$2.0e-4$	$1.960e-4$	$2.098e-4$
(0.8, 0.8)	$2.46e-4$	$2.0e-4$	$2.428e-4$	$2.034e-4$
(0.9, 0.9)	$2.29e-4$	$1.0e-4$	$1.776e-4$	$2.119e-4$

**Figure 1.** Plot of exact and approximate solutions at time $t = 0.5$ and $t = 0.9$ taking $\theta = 0, r = 5, J = 2$ and $\delta t = (0.1)/2^m$ for Example 1.

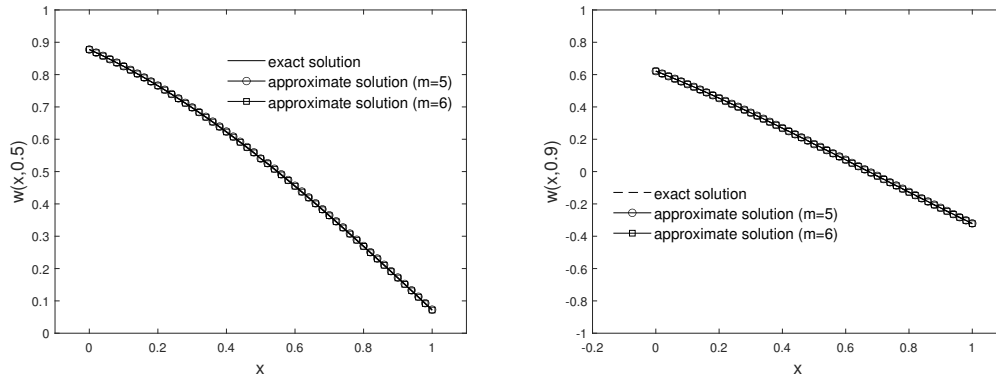


Figure 2. Plot of exact and approximate solutions at time $t = 0.5$ and $t = 0.9$ taking $\theta = 1/2, r = 5, J = 2$ and $\delta t = (0.1)/2^m$ for Example 1.

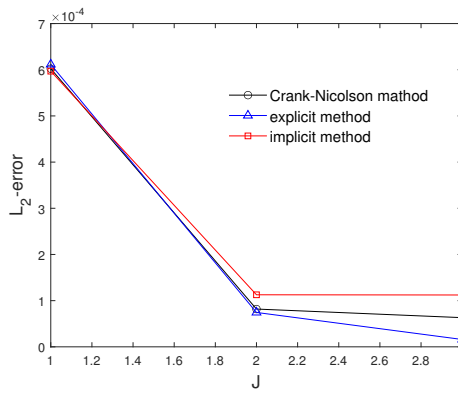


Figure 3. Plot of L_2 errors at time $t = 1$ taking $r = 3$ and $\delta t = (0.1)/2^9$ for Example 1.

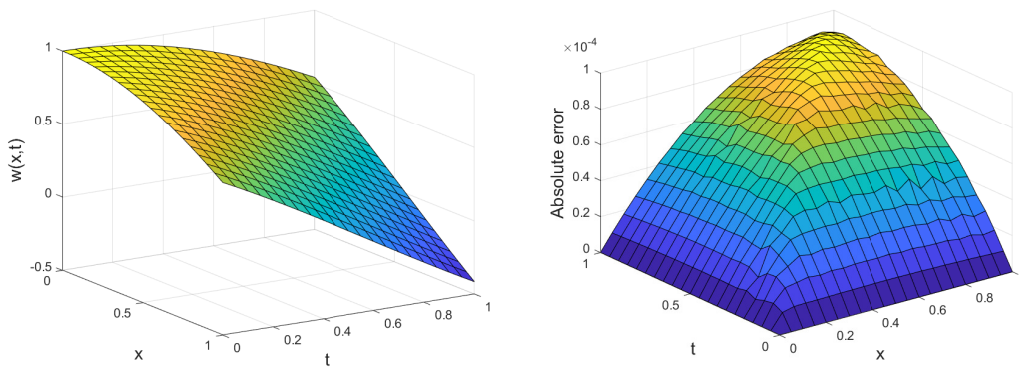


Figure 4. Plot of the approximate solution (left) and L_∞ errors (right) taking $r = 5$ and $J = 2$ for Example 1.

Table 5. L_2 -error comparison among explicit, implicit and Crank–Nicolson methods with time step size $\delta t = 0.1/2^{m-1}$ for Example 2.

θ	$m = 1$	$m = 2$	$m = 3$	$m = 4$	$m = 5$	$m = 6$	$m = 7$	$m = 8$	$m = 9$	$m = 10$
0	$2.37e + 4$	$8.67e + 6$	$6.20e + 7$	$1.51e + 5$	$5.88e - 0$	$2.68e - 3$	$6.44e - 4$	$3.21e - 4$	$1.60e - 4$	$8.01e - 5$
1/2	$1.45e - 2$	$7.25e - 3$	$3.62e - 3$	$1.81e - 3$	$9.06e - 4$	$4.53e - 4$	$2.27e - 4$	$1.13e - 4$	$5.66e - 5$	$2.83e - 5$
1	$2.46e - 2$	$1.23e - 2$	$6.13e - 3$	$3.06e - 3$	$1.53e - 3$	$7.65e - 4$	$3.82e - 4$	$1.91e - 4$	$9.55e - 5$	$4.78e - 5$

Table 6. L^2 norm of errors taking $r = 3, J = 2, \theta = 1/2$ and $\delta t = 0.1/2^{m-1}$ for Example 2.

m	$t = 0.2$	$t = 0.4$	$t = 0.6$	$t = 0.8$	$t = 1.0$
2	$3.75e - 3$	$4.50e - 3$	$3.97e - 3$	$4.58e - 3$	$7.27e - 3$
4	$9.37e - 4$	$1.12e - 3$	$9.91e - 4$	$1.14e - 3$	$1.82e - 3$
6	$2.34e - 4$	$2.81e - 4$	$2.48e - 4$	$2.86e - 4$	$4.55e - 4$
8	$5.85e - 5$	$7.02e - 5$	$6.20e - 5$	$7.15e - 5$	$1.14e - 4$
10	$1.46e - 5$	$1.76e - 5$	$1.55e - 5$	$1.79e - 5$	$2.84e - 5$

For this example we have the exact solution [16]

$$w(x, t) = (x - t)^2.$$

Table 5 shows the comparison of L_2 -error via explicit, implicit and Crank–Nicolson methods with time step size $\delta t = 0.1/2^{m-1}$, $m = 1, \dots, 10$, $r = 5$ and $J = 2$. Table 6 consist of L_2 norm of example 2 at different values of time. Figure 5 illustrate the approximate solution and absolute error taking $r = 5$ and $J = 2$ at time $t = 1$. Figure 6 shows the L_2 -error using explicit method and implicit method taking $r = 3$ and $J = 2$ at time $\delta t = 0.1/2^{m-1}$, $m = 1, \dots, 10$. Figures 7, 8 and 9 confirm our investigation about stability. Due to stability investigation, If the spectral radius of matrix $A^{-1}B$ is not less than 1, the time discretization leads to divergence when t increases. To reduce this effect, we must increase the time steps. The results have been compared with the Legendre wavelets and Chebyshev wavelet collocation method [16]. It shows that the proposed method offers better accuracy using same multiplicity parameter r and refinement level J . In Figure 10, we show the effect of refinement level J and time step size δt on absolute error. Also this Figure confirm our investigation about consistency.

5. Conclusions

This work is devoted to solving the one-dimensional partial differential equation with boundary and initial conditions. To this end, the desired equation reduces to an ordinary differential equation using the θ -weighted method. This ODE is solved by employing the Galerkin method based on the interpolating scaling functions. The stability, consistency, and convergency of the method are investigated. The numerical examples are reported to illustrate the accuracy and efficiency of the

Table 7. Absolute values of the error at the selected points taking $\theta = 1/2$ and $\delta t = 0.1/2^9$ for Example 1.

(x, t)	[16] ($M = M' = 4$)		Proposed method
	Legendre wavelets	Chebyshev wavelet	$r = 4, J = 1$
(0.1, 0.1)	$1.03e - 4$	$2.57e - 4$	$1.11e - 7$
(0.2, 0.2)	$9.00e - 6$	$3.83e - 4$	$1.09e - 7$
(0.3, 0.3)	$5.87e - 5$	$4.38e - 4$	$5.88e - 7$
(0.4, 0.4)	$9.94e - 5$	$2.22e - 5$	$1.30e - 6$
(0.5, 0.5)	$1.12e - 4$	$2.30e - 4$	$2.58e - 6$
(0.6, 0.6)	$9.94e - 5$	$1.38e - 5$	$7.09e - 7$
(0.7, 0.7)	$5.87e - 5$	$3.66e - 4$	$3.69e - 7$
(0.8, 0.8)	$9.00e - 6$	$2.75e - 4$	$3.73e - 8$
(0.9, 0.9)	$1.03e - 4$	$4.01e - 4$	$2.47e - 7$

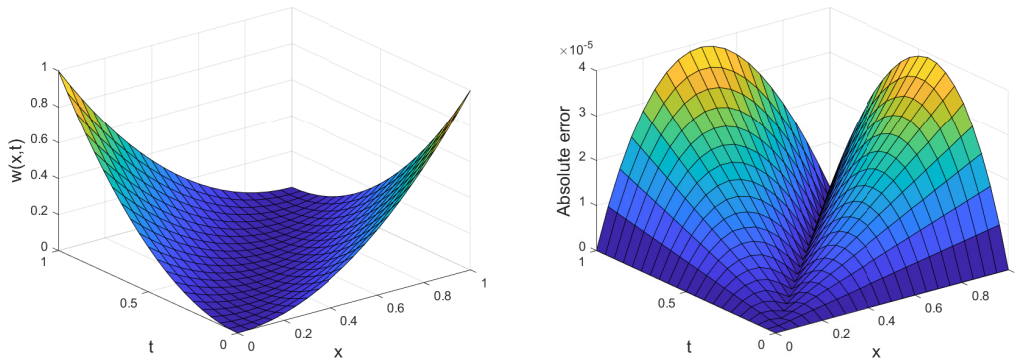


Figure 5. Plot of the approximate solution (left) and L_∞ errors (right) taking $r = 5$ and $J = 2$ for Example 2.

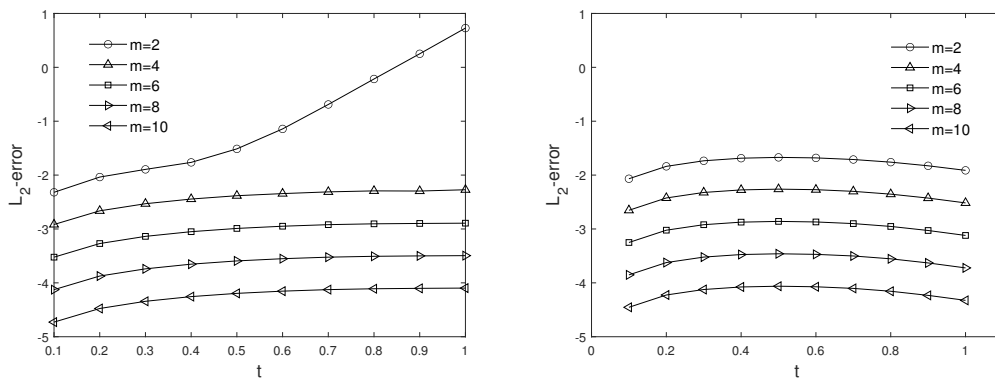


Figure 6. L_2 -error using explicit method (left) and implicit error (right) taking $r = 3$ and $J = 2$ at time $\delta t = 0.1/2^{m-1}$ for Example 2

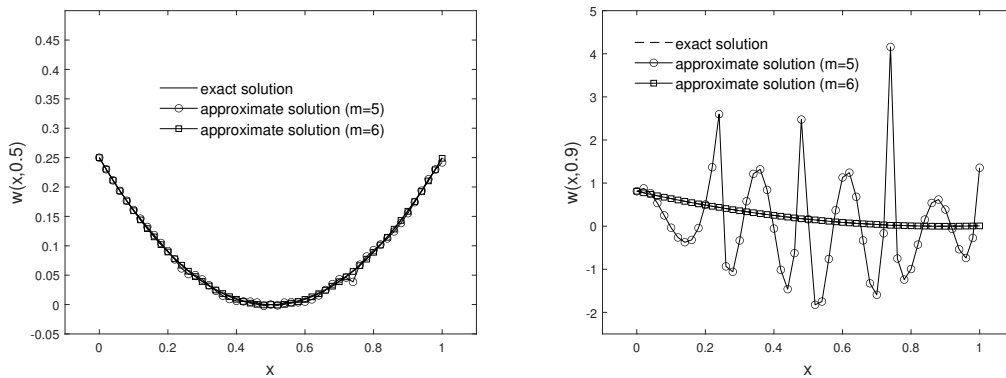


Figure 7. Plot of exact and approximate solutions at time $t = 0.5$ and $t = 0.9$ taking $\theta = 0, r = 5, J = 2$ and $\delta t = (0.1)/2^m$ for Example 2.

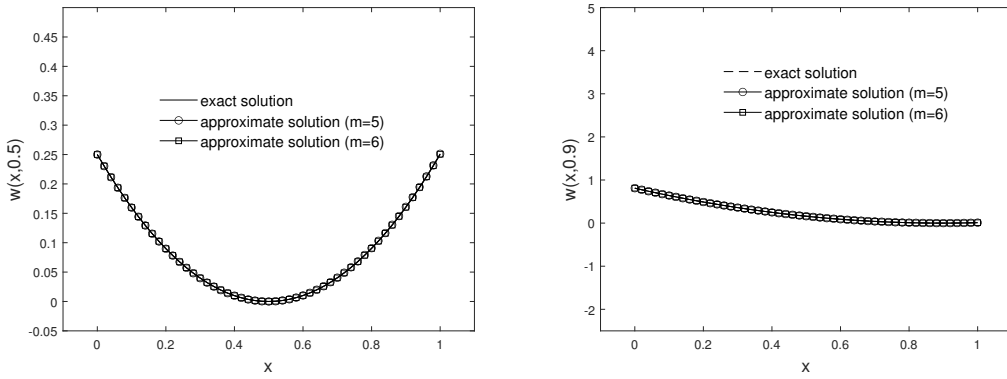


Figure 8. Plot of exact and approximate solutions at time $t = 0.5$ and $t = 0.9$ taking $\theta = 1/2$, $r = 5$, $J = 2$ and $\delta t = (0.1)/2^m$ for Example 2.

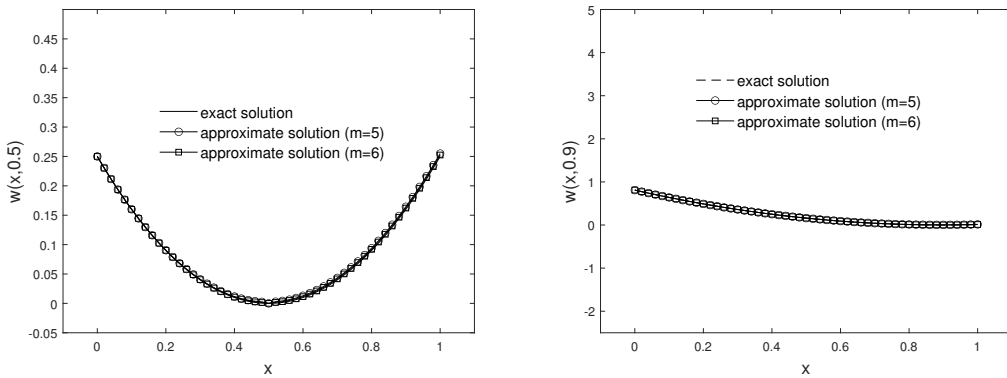


Figure 9. Plot of exact and approximate solutions at time $t = 0.5$ and $t = 0.9$ taking $\theta = 1$, $r = 5$, $J = 2$ and $\delta t = (0.1)/2^m$ for Example 2.

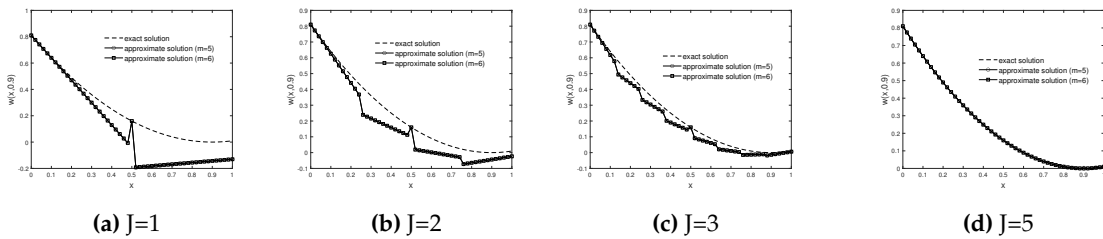


Figure 10. Effect of the refinement level J and δt on the absolute error for Example 2.

113 method. The results show that three parameters are important here, the θ parameter that changes
 114 the θ -weighted method, the δt parameter that controls the time steps, and the refinement level J .
 115 The results show that using the proposed method better results are obtained compared to similar
 116 methods. Among the methods utilized in this paper, the implicit and Crank–Nicolson methods are
 117 stable methods that need fewer steps than the explicit method to achieve proper accuracy.

118 **Author Contributions:** Conceptualization, H.B.J.; methodology, software, H.B.J. and F.T; validation, formal
 119 analysis, H.B.J. and F.T; writing–original draft preparation, investigation, funding acquisition, H.B.J. and F.T;
 120 writing–review and editing, H.B.J. and F.T. All authors have read and agreed to the published version of the
 121 manuscript.

122 **Funding:** The authors extend their appreciation to the Deanship of Scientific Research at King Saud University
 123 for funding this work through research group no. RG-1441-326.

124 **Conflicts of Interest:** The authors declare no conflict of interest.

125 Abbreviations

126 The following abbreviations are used in this manuscript:

127	HPDE	Hyperbolic partial differential Equations
	ISFs	Interpolating scaling functions
128	PDEs	Partial differential equations
	ODE	Ordinary differential equation

129 References

- 130 1. B. Alpert; G. Beylkin; D. Gines; L. Vozovoi. Adaptive solution of partial differential equations in multiwavelet
 131 bases. *J. Comput. Phys.* **2002**, *182*, 149–190.
- 132 2. B. Alpert; G. Beylkin; R. R. Coifman; V. Rokhlin. Wavelet-like bases for the fast solution of second-kind
 133 integral equations. *SIAM J. Sci. Statist. Comput.* **1993**, *14(1)*, 159–184.
- 134 3. L. Bougoffa. An efficient method for solving nonlocal initial-boundary value problems for linear and
 135 nonlinear first-order hyperbolic partial differential equations. *J. Appl. Math. Comput.* **2013**, *43*, 31–54.
- 136 4. M. Dehghan. A computational study of the one-dimensional parabolic equation subject to nonclassical
 137 boundary specifications. *Numer. Meth. Part. D. E.* **2006**, *22*, 220–257.
- 138 5. M. Dehghan; M. Lakesatani. The Use of Cubic B-Spline Scaling Functions for Solving the One-dimensional
 139 Hyperbolic Equation with a Nonlocal Conservation Condition. *Numer. Math. Part. D. E.* **2007**, *23(6)*,
 140 1277–1289.
- 141 6. A. Saadatmandi; M. Dehghan. Numerical solution of hyperbolic telegraph equation using the Chebyshev
 142 Tau method. *Numer. Meth. Part. D. E.* **2010**, *26(1)*, 239–252.
- 143 7. M. Dehghan; A. Shokri. A numerical method for solving the hyperbolic telegraph equation. *Numer. Meth.*
 144 *Part. D. E.* **2008**, *24(4)*, 1080–1093.
- 145 8. E.H. Doha; A.H. Bhrawy; R.M. Hafez; M.A. Abdelkawy. A Chebyshev–Gauss–Radau scheme for nonlinear
 146 hyperbolic system of first order. *Appl. Math. Inf. Sci.* **2014**, *8(2)*, 535–544.
- 147 9. E.H. Doha; R.M. Hafez; Y.H. Youssri. Shifted Jacobi spectral–Galerkin method for solving hyperbolic partial
 148 differential equations. *Comput. Math. Appl.* **2019**, *78(3)*, 889–904.
- 149 10. H. Bin Jebreen; Y. Chalco Cano; I. Dassios. An efficient algorithm based on the multi-wavelet Galerkin
 150 method for telegraph equation. *AIMS Mathematics* **2021**, *6(2)*, 1296–1308.
- 151 11. M. Lakestani; B. N. Saray. Numerical solution of telegraph equation using interpolating scaling functions.
 152 *Comput. Math. Appl.* **2010**, *60*, 1964–1972.
- 153 12. B.N. Saray. Sparse multiscale representation of Galerkin method for solving linear-mixed Volterra–Fredholm
 154 integral equations. *Math. Methods Appl. Sci.* **2020**, *43(5)*, 2601–2614.
- 155 13. B.N. Saray; J. Manafian. Sparse representation of delay differential equation of pantograph type using
 156 multiwavelets Galerkin method. *Eng. Computation.* **2018**, *35(2)*, 887–903.
- 157 14. S. H. Seyed; B. N. Saray; A. Ramazani. High-Accuracy Multiscale Simulation of Three-Dimensional
 158 Squeezing Carbon Nanotube-Based Flow inside a Rotating Stretching Channel. *Math. Prob. Eng.* **2019**, *2019*,
 159 1–18.

- 160 15. M. Shahriari; B.N. Saray; M. Lakestani; J. Manafian. Numerical treatment of the Benjamin-Bona-Mahony
161 equation using Alpert multiwavelets. *Eur. Phys. J. Plus.* **2018**, *133*, 1–12.
- 162 16. S. Singh; V.K. Patel; V.K. Singh. Application of wavelet collocation method for hyperbolic partial differential
163 equations via matrices. *Appl. Math. Comput.* **2018**, *320(1)*, 407–424.
- 164 17. E. Tohidi; F. Toutounian. Convergence analysis of Bernoulli matrix approach for one-dimensional matrix
165 hyperbolic equations of the first order. *Comput. Math. Appl.* **2014**, *68*, 1–12.

166 **Publisher’s Note:** MDPI stays neutral with regard to jurisdictional claims in published maps and institutional
167 affiliations.

168 © 2020 by the authors. Submitted to *Journal Not Specified* for possible open access publication
169 under the terms and conditions of the Creative Commons Attribution (CC BY) license
170 (<http://creativecommons.org/licenses/by/4.0/>).